AIP Applied Physics Letters

Effects of phosphorus doping by plasma immersion ion implantation on the structural and optical characteristics of Zn0.85Mg0.15O thin films

S. Saha, S. Nagar, and S. Chakrabarti

Citation: Applied Physics Letters **105**, 061109 (2014); doi: 10.1063/1.4893138
View online: http://dx.doi.org/10.1063/1.4893138
View Table of Contents: http://scitation.aip.org/content/aip/journal/apl/105/6?ver=pdfcov
Published by the AIP Publishing

Articles you may be interested in
Structure and optical properties of a-plane ZnO/Zn0.9Mg0.1O multiple quantum wells grown on r-plane sapphire substrates by pulsed laser deposition
J. Appl. Phys. **112**, 103519 (2012); 10.1063/1.4767462

Effect of (O, As) dual implantation on p-type doping of ZnO films
J. Appl. Phys. **110**, 103708 (2011); 10.1063/1.3662908

Quenching of surface-exciton emission from ZnO nanocombs by plasma immersion ion implantation
Appl. Phys. Lett. **91**, 071921 (2007); 10.1063/1.2772668

Effect of phosphorus dopant on photoluminescence and field-emission characteristics of Mg 0.1 Zn 0.9 O nanowires
J. Appl. Phys. **99**, 024303 (2006); 10.1063/1.2161420

Realization of Mg (x = 0.15) Zn (1 − x = 0.85) O -based metal-semiconductor-metal UV detector on quartz and sapphire
J. Vac. Sci. Technol. A **23**, 982 (2005); 10.1116/1.1913677

This article is copyrighted as indicated in the article. Reuse of AIP content is subject to the terms at: http://scitation.aip.org/termsconditions. Downloaded to IP: 128.114.34.22 On: Tue, 02 Dec 2014 03:17:54

APPLIED PHYSICS LETTERS 105, 061109 (2014)

Effects of phosphorus doping by plasma immersion ion implantation on the structural and optical characteristics of $Zn_{0.85}Mg_{0.15}O$ thin films

S. Saha, S. Nagar, and S. Chakrabarti[a)]
Department of Electrical Engineering, Indian Institute of Technology Bombay, Powai, Mumbai 400076, India

(Received 26 June 2014; accepted 22 July 2014; published online 12 August 2014)

ZnMgO thin films deposited on ⟨100⟩ Si substrates by RF sputtering were annealed at 800, 900, and 1000 °C after phosphorus plasma immersion ion implantation. X-ray diffraction spectra confirmed the presence of $\langle 10\bar{1}0\rangle$ and $\langle 10\bar{1}3\rangle$ peaks for all the samples. However, in case of the annealed samples, the ⟨0002⟩ peak was also observed. Scanning electron microscopy images revealed the variation in surface morphology caused by phosphorus implantation. Implanted and non-implanted samples were compared to examine the effects of phosphorus implantation on the optical properties of ZnMgO. Optical characteristics were investigated by low-temperature (15 K) photoluminescence experiments. Inelastic exciton–exciton scattering and localized, and delocalized excitonic peaks appeared at 3.377, 3.42, and 3.45 eV, respectively, revealing the excitonic effect resulting from phosphorus implantation. This result is important because inelastic exciton–exciton scattering leads to nonlinear emission, which can improve the performance of many optoelectronic devices. © *2014 AIP Publishing LLC*. [http://dx.doi.org/10.1063/1.4893138]

The excitonic property of wide bandgap semiconductors makes them suitable for use in optoelectronic devices and related applications. The interaction between excitons produces biexcitons and inelastic scattering, which in turn leads to nonlinear emission.[1] Owing to its large exciton binding energy of 60 meV and a direct bandgap of approximately 3.4 eV at room temperature, Zinc oxide (ZnO) has been widely considered for use in optoelectronic devices such as short-wavelength laser diodes and blue and ultraviolet (UV) light-emitting diodes.[2–7] One-dimensional ZnO nanowires are suitable for chemical-biological agent detection and solid-state lighting.[8] The piezoelectric properties of ZnO make it suitable for electroacoustic applications such as in SONAR emitters and detectors.[9] Modulation of the bandgap can further enhance the performance of ZnO devices. This can be achieved by the controlled mixing of ZnO ($E_g \approx 3.4$ eV) with MgO ($E_g \approx 7.8$ eV), which yields $Zn_{1-x}Mg_xO$.[10–12] However, ZnO and MgO have completely different crystal structures: ZnO exhibits a wurtzite structure with hexagonal symmetry ($a = 3.24$ Å and $b = 5.20$ Å), while MgO exhibits a rock salt structure with cubic symmetry ($a = 4.24$ Å).[13] As a result, alloying these materials in imprecise proportions may lead to a lattice mismatch. Further, to avoid phase segregation, the molar fraction of Mg cannot be increased above 33%–40%.[14–17]

This report examines the effect of phosphorus implantation on the structural and optical properties of ZnMgO thin films. We have previously reported on p-type ZnO films implanted with phosphorus by plasma immersion ion implantation (PIII).[18,19] The same approach has extended to ZnMgO thin films in an attempt to achieve reliable and reproducible p-type films. Although a dominating acceptor peak was not detected, the implantation of phosphorus ions into $Zn_{1-x}Mg_xO$ by PIII shows promise. The detection of an inelastic exciton–exciton (XX) scattering peak, as well as localized (L) and delocalized (B) exciton peaks in the case of the phosphorus-implanted samples, suggests that ZnMgO is a promising candidate for fabricating optoelectronic devices in the UV region. The excitonic effect narrows the optical gain, resulting in a lasing process with high gain and a low threshold.[1]

A thin $Zn_{1-x}Mg_xO$ ($x = 0.15$) film with a thickness of 190 nm was grown on an n-type ⟨100⟩ highly resistive (500 Ω cm) silicon wafer by RF sputtering. A 99.999% pure $Zn_{0.85}Mg_{0.15}O$ target was deposited for 30 min with an RF power of 100 W. The RCA-cleaned silicon substrate was dipped in 2% HF (192 ml de-ionised (DI) water and 8 ml HF) for 30 s prior to deposition. Deposition was performed in a high-vacuum chamber under ambient argon pressure of 2.2×10^{-2} mbar (sample A). Figure 1 shows a representative cross-sectional scanning electron microscopy (SEM) image of

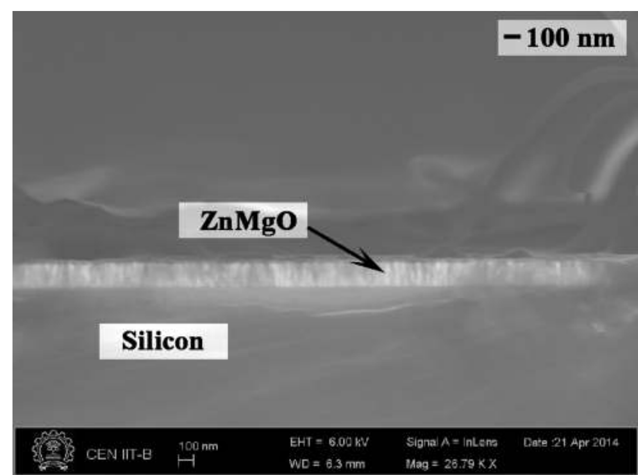

FIG. 1. Cross-sectional SEM image of the implanted sample, confirming a continuous film on the Si substrate.

a)Author to whom correspondence should be addressed. Electronic mail: subho@ee.iitb.ac.in.

 © 2014 AIP Publishing LLC

This article is copyrighted as indicated in the article. Reuse of AIP content is subject to the terms at: http://scitation.aip.org/termsconditions. Downloaded to IP: 128.114.34.22 On: Tue, 02 Dec 2014 03:17:54

one of the samples, from which the film thickness was measured, and the continuity of the film throughout the Si surface was confirmed.

The as-grown sample was subjected to phosphorus implantation by PIII to obtain sample P1. A high negative pulse of -2 kV was applied to the sample for 30 s. The RF was fixed at 5 kHz with an ON time of 10 μs. The applied RF plasma power of 900 W created phosphorus plasma from phosphine gas. The chamber pressure was maintained at 0.1 mbar during implantation. The samples were subsequently subjected to rapid thermal annealing (Annealsys AS ONE 150) in ambient oxygen for 10 s at 800, 900, and 1000 °C to remove implantation-related defects, yielding samples P2, P3, and P4, respectively. To study the effect of phosphorus implantation, sample A was also annealed at similar conditions to obtain samples B, C, and D.

The structural properties of the obtained samples were analyzed by x-ray diffraction (XRD) with CuKα1 radiation and SEM. Optical characteristics of the films were investigated by low-temperature (15 K) photoluminescence (PL) experiments using a He–Cd laser with a wavelength of 325 nm as the excitation source, and spectra were recorded using a Si detector array.

The XRD profile of the obtained films is shown in Fig. 2. Diffraction peaks at 2θ angles of 32.9° and 61.5° corresponding to $\langle 10\bar{1}0\rangle$ and $\langle 10\bar{1}3\rangle$ were observed for all samples. Moreover, the $\langle 0002\rangle$ peak at 34.5° was also observed for the annealed samples, which suggests that annealing makes the films more c-axis oriented. We noted that the $\langle 10\bar{1}3\rangle$ peak was the dominant peak. Increasing the annealing temperature increased the intensity of the film because high-temperature annealing reduces the number of defects; the presence of oxygen during annealing improves the crystallinity of the film, resulting in higher intensity. Uniform lattice constants of a = 3.175 Å and c = 2.768 Å were obtained for all samples annealed at different temperatures on the basis of Eq. (1) and Bragg's law

$$(1/d_{hkl}^2) = (4/3)([h^2 + k^2 + hk]/a^2) + (l^2/c^2). \quad (1)$$

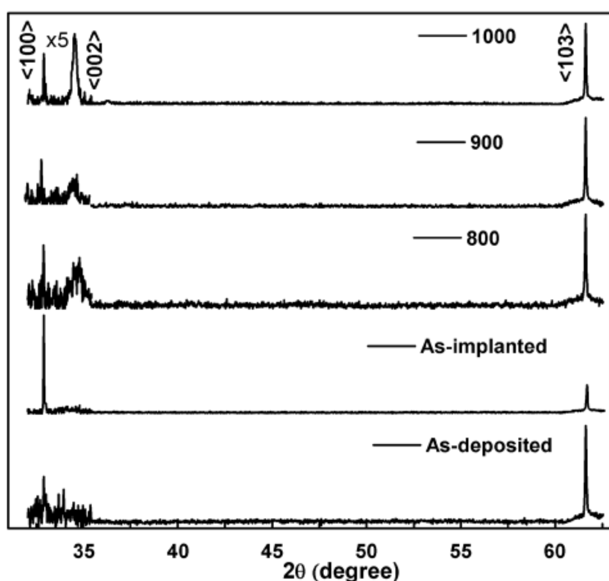

FIG. 2. XRD profile images of various samples.

TABLE I. FWHM and grain size of as-grown and as-implanted samples as well as those annealed at 800, 900, and 1000 °C.

Sample	FWHM	Grain size (nm)
As-grown	0.076	40.22
As-implanted	0.079	38.56
800 °C	0.078	39.04
900 °C	0.070	43.50
1000 °C	0.072	42.30

Here, h, k, and l are the Miller indices, d is the distance between two adjacent planes, and a and c are the primitive lattice vectors.

The full-width at half-maximum (FWHM) values of the $\langle 10\bar{1}3\rangle$ peak are shown in Table I. The FWHM of the as-implanted sample was higher than that of the as-deposited one because of enhanced defects in the films caused by implantation. However, on annealing, the FWHM values decreased, indicating that the defects diminish.

Surface analysis of the obtained thin films was performed by SEM (Fig. 3). Dense grains were clearly observed in the as-deposited samples, while the as-implanted samples had scattered grains and more defects, clearly indicating that implantation leads to some surface damage. However, on annealing, the defects in the implanted sample reduced and denser grains began to form. On annealing the sample at 1000 °C, the denser grains were clearly visible along with a larger grain size. The high temperature may have caused the smaller grains to merge and form larger ones. Thus, the defects caused by implantation decreased, leading to better quality films; this observation was further confirmed by the low FWHM values of the annealed samples obtained from XRD.

Low-temperature (15 K) PL experiments were conducted to analyze the effects of phosphorus implantation on

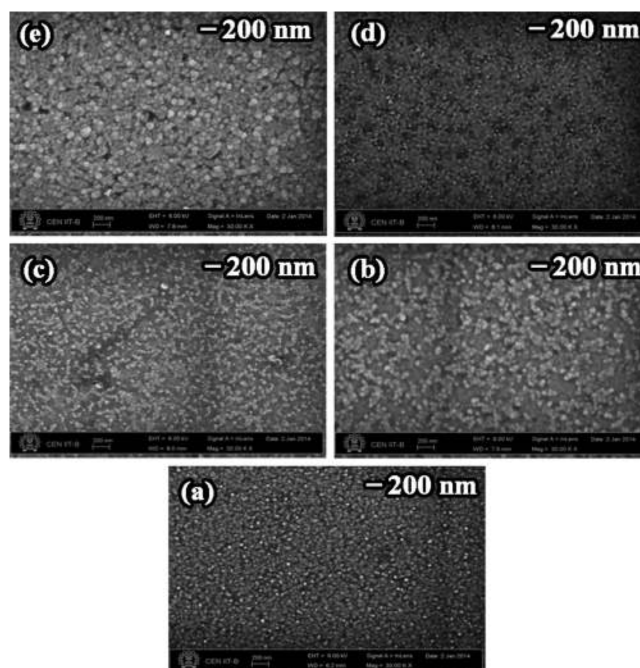

FIG. 3. SEM images of the (a) as-grown sample, (b) as-implanted sample, and samples annealed at (c) 800, (d) 900, and (e) 1000 °C.

This article is copyrighted as indicated in the article. Reuse of AIP content is subject to the terms at: http://scitation.aip.org/termsconditions. Downloaded to IP: 128.114.34.22 On: Tue, 02 Dec 2014 03:17:54

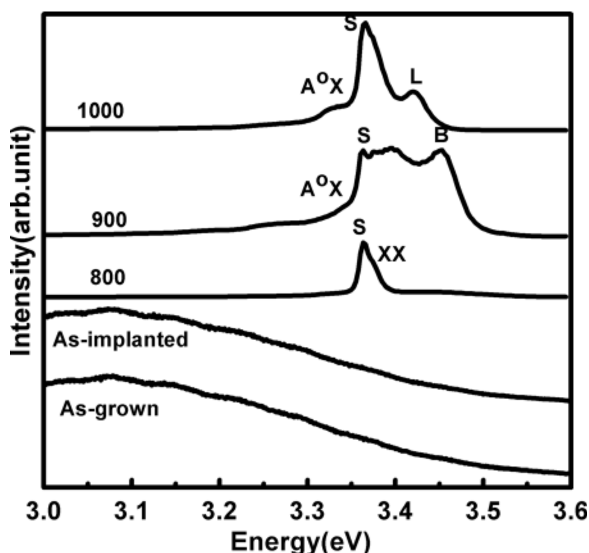

FIG. 4. Photoluminescence spectra of the implanted samples showing the various peaks at 15 K.

the thin-film optical properties (Fig. 4). Figure 5 shows the PL spectra of the as-deposited and annealed samples. Near-band edge emission was not observed for either as-deposited or as-implanted samples because of the increased deep-level defects. A dominant peak around 3.364 eV was observed in the case of the implanted samples after annealing at 800, 900, and 1000 °C, which was not observed in the case of the as-annealed samples. This peak, denoted as the S-peak, is close to the donor-bound exciton peak for ZnO, and is likely the result of phosphorus implantation (Figure 4).[20] The reduction in the Mg content in the film because of the combined effect of annealing and implantation may have led to the appearance of this peak. However, further investigation is needed to ascertain the exact origin of this peak. Another important observation from the spectra of the implanted samples was the occurrence of the inelastic XX scattering peak around 3.377 eV.[1,21] The dynamics of the excitons can be explained by either an external pump or relaxation process, which causes an energy exchange between the excitons, or

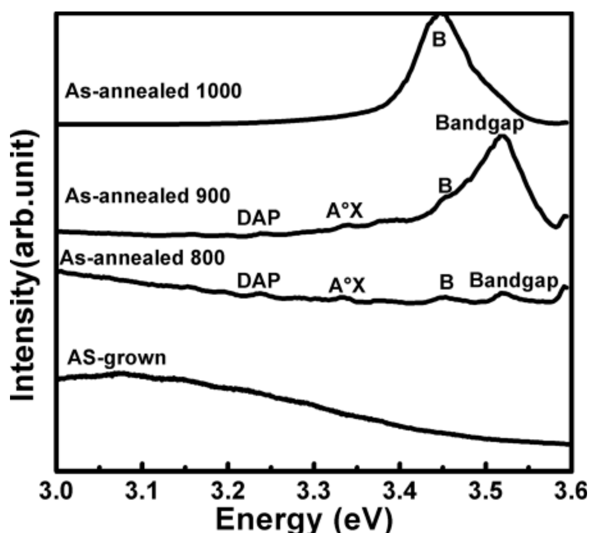

FIG. 5. Photoluminescence spectra of the as-annealed samples showing the various peaks at 15 K.

by the radiative recombination process.[22] Given that ZnO is a direct bandgap semiconductor, radiative recombination seems like a plausible explanation for the appearance of the XX scattering peak in ZnMgO. However, if radiative recombination led to the appearance of the XX peak, it should have also appeared in the as-annealed samples. Another possibility is that an exciton gets trapped at a shallow-level site, resulting in a bound exciton. This is the most likely explanation because phosphorus acting as a p-type dopant in ZnMgO might lead to the formation of shallow levels. This scattering plays an important role in the emission of lasing, which is observed in ZnO-based quantum well structures. To fabricate ZnO-based light-emitting devices, XX scattering is an important factor.[23] The emission of lasing is mainly caused by two processes: LO-phonon-assisted recombination and XX scattering. The XX scattering process can be described as follows:

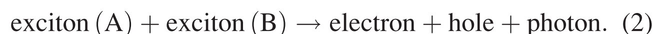

$$\text{exciton}\,(A) + \text{exciton}\,(B) \rightarrow \text{electron} + \text{hole} + \text{photon}. \quad (2)$$

The energy conservation condition for this process is as follows:

$$\hbar\omega_p = E_g - 2E_{ex} - \delta E_{kin} + E_{kin}{}^{ex(A)} + E_{kin}{}^{ex(B)}. \quad (3)$$

Here, E_g, E_{ex}, δE_{kin}, $E_{kin}{}^{ex(A)}$, and $E_{kin}{}^{ex(B)}$ are the bandgap, exciton binding energy, kinetic energy of the free electrons and holes resulting from the process, and kinetic energy of excitons A and B, respectively. If the lowest conduction and the highest valence bands are not filled and the kinetic energy of the excitons is sufficiently small at the lasing threshold, then $\delta E_{kin} = 0$, and

$$\Delta E_{laser}{}^{th} = E_{ex}. \quad (4)$$

Increasing the excitation intensity causes the conduction and valence bands to be filled with free carriers.[24] This suggests that phosphorus implantation leads to an excitonic process, which can play an important role in the fabrication of devices such as low-threshold lasers.[25]

A peak at 3.452 eV was observed for the sample annealed at 900 °C, which can be attributed to the delocalized exciton; this peak was also observed in as-annealed samples.[20,26,27] In the case of the implanted sample annealed at 1000 °C, this peak was replaced by the localized exciton peak around 3.422 eV.[20,26,27] The difference between the localized and delocalized excitons can be described in terms of the wave function. The wave function of a delocalized exciton is always a propagating wave, while that of a localized exciton decays with distance.[28] The implantation of phosphorus ions followed by high-temperature annealing may have led to increased localized states, resulting in the disappearance of the delocalized states.

The implanted samples exhibited another small peak around 3.337 eV, which was identified as the acceptor-bound exciton (A°X) peak. The as-annealed samples also exhibited this peak along with a donor-to-acceptor pair (DAP) peak around 3.24 eV.[29] After implantation, the DAP peak completely disappeared, while the intensity of the A°X peak increased in the samples annealed at 900, and 1000 °C. The incorporation of phosphorus ions introduces more acceptors

This article is copyrighted as indicated in the article. Reuse of AIP content is subject to the terms at: http://scitation.aip.org/termsconditions. Downloaded to IP: 128.114.34.22 On: Tue, 02 Dec 2014 03:17:54

in the film, thus suppressing the DAP peak and enhancing the A°X peak. The A°X peak was seen in samples annealed at high temperature, possibly because of an increase of acceptors in the films from phosphorus implantation.

A comprehensive analysis of the structural and low-temperature optical properties of phosphorus-implanted $Zn_{0.85}Mg_{0.15}O$ was conducted. XRD diffraction spectra showed the existence of $\langle 10\bar{1}0\rangle$ and $\langle 10\bar{1}3\rangle$ peaks for all samples. Notably, the $\langle 0002\rangle$ peak was also observed in the case of the annealed samples, indicating that the films become more c-axis oriented. Low-temperature PL measurements of the implanted samples showed the inelastic exciton–exciton scattering peak as well as localized and delocalized exciton peaks. The absence of these peaks in the as-annealed samples confirms that phosphorus implantation leads to an increase in excitons in the ZnMgO thin films. The presence of these excitonic effects is useful for designing high-frequency optical devices such as lasers using ZnMgO, operating in the UV region.

S.S., S.N., and S.C. would like to acknowledge financial support provided by the Department of Science and Technology, India, as well as partial financial support provided by the Department of Information Technology, Government of India, through the Centre of Excellence in Nanoelectronics. They would also like to thank A. K. Ray and Professor R. Pinto for their contribution to the research.

[1]C. H. Chia, J. N. Chen, and Y. M. Hu, Appl. Phys. Lett. **99**, 131908 (2011).
[2]D. C. Reynolds, C. W. Litton, T. C. Collins, J. E. Hoelscher, and J. Nause, Appl. Phys. Lett. **88**, 141919 (2006).
[3]B. Rakshit and P. Mahadevan, Appl. Phys. Lett. **102**, 143116 (2013).
[4]C. Klingshirn, Phys. Status Solidi B **244**, 3027 (2007).
[5]M. D. Neumann, C. Cobet, N. Esser, B. Laumer, and T. A. Wassner, J. Appl. Phys. **110**, 013520 (2011).
[6]P. Erhart, K. Albe, and A. Klein, Phys. Rev. B **73**, 205203 (2006).
[7]Ü. Özgür, Y. I. Alivov, C. Liu, A. Teke, M. A. Reshchiko, S. Doğan, V. Avrutin, S.-J. Cho, and H. Morkoç, J. Appl. Phys. **98**, 041301 (2005).
[8]H. C. Hsu, C. Y. Wu, C. Hsin-Ming, and W. F. Hsieh, Appl. Phys. Lett. **89**, 013101 (2006).
[9]O. Lopatiuk, W. Burdett, L. Chernyak, K. P. Ip, Y. W. Heo, D. P. Norton, S. J. Pearton, B. Hertog, P. P. Chow, and A. Osinsky, Appl. Phys. Lett. **86**, 012105 (2005).
[10]T. Z. Raza, J. I. Cerda, and H. J. Raza, J. Appl. Phys. **109**, 023705 (2011).
[11]M. Trunk, V. Venkatachalapathy, A. Galeckas, and A. Y. Kuznetsov, Appl. Phys. Lett. **97**, 211901 (2010).
[12]V. V. Sobolev, Inorg. Mater. **40**, 1169 (2004).
[13]Y. S. Chang, C. T. Chien, C. W. Chen, T. Y. Chu, and H. H. Chiang, J. Appl. Phys. **101**, 033502 (2007).
[14]M. Heinemann and C. Heiliger, J. Appl. Phys. **110**, 083103 (2011).
[15]Y. Ke, J. Berry, P. Parilla, A. Zakutayev, R. O'Hayre, and D. Ginley, Thin Solid Films **520**, 3697 (2012).
[16]A. Ohtomo, M. Kawasaki, T. Koida, K. Masubuchi, H. Koinuma, Y. Sakurai, Y. Yoshida, T. Yasuda, and Y. Segawa, Appl. Phys. Lett. **72**, 2466 (1998).
[17]T. Gruber, C. Kirchner, R. Kling, F. Reuss, A. Waag, F. Bertram, D. Forster, J. Christen, and M. Schreck, Appl. Phys. Lett. **83**, 3290 (2003).
[18]S. Nagar and S. Chakrabarti, J. Lumin. **137**, 55 (2013).
[19]S. Nagar and S. Chakrabarti, Proc. SPIE **8626**, 86261O (2013).
[20]A. L. Yang, H. P. Song, D. C. Liang, H. Y. Wei, X. L. Liu, P. Jin, X. B. Qin, S. Y. Yang, Q. S. Wang, and Z. G. Wang, Appl. Phys. Lett. **96**, 151904 (2010).
[21]H. D. Sun, T. Makino, Y. Segawa, M. Kawasaki, A. Ohtomo, K. Tamura, and H. Koinuma, Appl. Phys. Lett. **78**, 3385 (2001).
[22]F. Tassone and Y. Yamamoto, Phys. Rev. B **59**, 10830 (1999).
[23]H. D. Sun, T. Makino, N. T. Tuan, Y. Segawa, Z. K. Tang, G. K. L. Wong, M. Kawasaki, A. Ohtomo, K. Tamura, and H. Koinuma, Appl. Phys. Lett. **77**, 4250 (2000).
[24]Y. Kawakami, I. Hauksson, H. Stewart, J. Simpson, I. Galbraith, K. A. Prior, and B. C. Cavenett, Phys. Rev. B **48**, 11994 (1993).
[25]M. Asada, Y. Miamoto, and Y. Suematsu, IEEE J. Quantum Electron. **22**, 1915 (1986).
[26]H. Zhu, C. X. Shan, B. H. Li, Z. Z. Zhang, J. Y. Zhang, B. Yao, D. Z. Shen, and X. W. Fan, J. Appl. Phys. **105**, 103508 (2009).
[27]B. Laumer, T. A. Wassner, F. Schuster, M. Stutzmann, J. Schörmann, M. Rohnke, A. Chernikov, V. Bornwasser, M. Koch, S. Chatterjee, and M. J. Eickhoff, J. Appl. Phys. **110**, 093513 (2011).
[28]J. Hegarty, L. Goldner, and M. D. Struge, Phys. Rev B **30**, 7346 (1984).
[29]J. C. Fan, C. Y. Zhu, B. Yang, S. Fung, C. D. Beling, G. Brauer, W. Anwand, D. Grambole, W. Skorupa, K. S. Wong, Y. C. Zhong, Z. Xie, and C. C. Ling, J. Vac. Sci. Technol. A **29**, 03A103 (2011).

This article is copyrighted as indicated in the article. Reuse of AIP content is subject to the terms at: http://scitation.aip.org/termsconditions. Downloaded to IP: 128.114.34.22 On: Tue, 02 Dec 2014 03:17:54